Article:
Mangner, N, Garbade, J, Heyne, E et al. (2021) Molecular Mechanisms of Diaphragm Myopathy in Humans with Severe Heart Failure. Circulation Research. ISSN: 0009-7330

https://doi.org/10.1161/circresaha.120.318060

Molecular mechanisms of diaphragm myopathy in humans with severe heart failure

Norman Mangner[a], MD, Jens Garbade[b], MD, Estelle Heyne[c], PhD, Marloes van den Berg[d], MD, Ephraim B. Winzer[a], MD, Jennifer Hommel[a], MA, Marcus Sandri[e], MD, Joanna Jozwiak-Nozdrzykowska[e], MD, Anna L. Meyer[f], MD, Sven Lehmann[b], MD, Clara Schmitz[a], cand. med., Edoardo Malfatti[g], MD, Michael Schwarzer[c], PhD, Coen A. C. Ottenheijm[d], PhD, T. Scott Bowen[h], PhD, Axel Linke[a, i]*, MD, Volker Adams[a, i]*, PhD

* shared senior authorship

[a] Herzzentrum Dresden, Technische Universität Dresden, Department of Internal Medicine and Cardiology, Dresden, Germany
[b] Heart Center Leipzig – University Hospital, Department of Cardiac Surgery, Leipzig, Germany
[c] Jena University Hospital – Friedrich Schiller University of Jena, Department of Cardiothoracic Surgery, Jena, Germany
[d] Department of Physiology, Amsterdam UMC (location VUmc), Amsterdam, The Netherlands
[e] Heart Center Leipzig – University Hospital, Department of Cardiology, Leipzig, Germany
[f] Department of Cardiac Surgery, Heart and Marfan Center, University of Heidelberg, Heidelberg, Germany
[g] Neurology Department, Centre de Référence Maladies Neuromusculaires Nord-Est-Ile-de-France, CHU Raymond-Poincaré, Garches, France; U1179 UVSQ-INSERM, Université Versailles-Saint-Quentin-en-Yvelines, France
[h] School of Biomedical Sciences, Faculty of Biological Sciences, University of Leeds, Leeds, UK
[i] Dresden Cardiovascular Research Institute and Core Laboratories GmbH, Dresden, Germany

Running title: Heart Failure associated Diaphragm Dysfunction

Address for correspondence
Norman Mangner
Herzzentrum Dresden – Technische Universität Dresden
Department of Internal Medicine and Cardiology
Fetscherstr. 76
01307 Dresden / Germany
Tel: +49 351 45025297
E-mail: norman.mangner@tu-dresden.de

Word count
8372/8000

Subject Codes
Translational Studies; Pathophysiology; Oxidant Stress

Abstract:

Rationale: Diaphragm weakness impairs quality-of-life, exercise capacity, and survival in patients with chronic heart failure (CHF) and reduced left ventricular ejection fraction. However, the underlying cellular mechanisms responsible in humans remain poorly resolved.

Objectives: We prospectively evaluated clinical, functional (*in vivo*/*in vitro*), histological/ultrastructural and molecular alterations of the diaphragm from CHF patients receiving a left ventricular assist device compared to patients without CHF undergoing elective coronary bypass grafting (control) in the observational LIpsia DiaPhrAgm and MUScle Heart Failure Trial (LIPAMUS-HF).

Methods and Results: Participants (Controls=21, CHF=18) underwent cardiopulmonary exercise and spirometry/respiratory muscle testing alongside diaphragm and cardiac imaging. Diaphragm biopsies were phenotyped for mitochondrial respiration, muscle fiber function, histology/ultrastructure, and protein expression.

In vivo respiratory muscle function and diaphragm thickness were reduced in CHF by 38% and 23%. Diaphragm biopsies revealed a fiber-type shift and severe fiber atrophy in CHF alongside elevated proteasome-dependent proteolysis (i.e., MuRF1 expression, ubiquitination, ubiquitin proteasome activity) and myofibrillar protein oxidation, which corresponded to upregulated NADPH oxidase (Nox2/Nox4) signaling. Mitochondria demonstrated severe intrinsic functional and ultrastructural abnormalities in CHF characterized by accumulation of small mitochondria and inhibited autophagy/mitophagy. Single muscle fiber contractile function revealed reduced Ca^{2+} sensitivity in CHF and there was evidence of ryanodine receptor 1 (RyR1) dysfunction indicating Ca^{2+} leak from the sarcoplasmatic reticulum. Mitochondrial and Ca^{2+} measures corresponded to upregulated Nox4 isoform NADPH oxidase expression. Molecular markers correlated to whole-body exercise intolerance and diaphragm dysfunction/wasting.

Conclusions: CHF patients demonstrate an obvious diaphragm myopathy independent of disuse or other confounding factors such as ageing, obesity, or hypertension. Diaphragm weakness in CHF was associated with intracellular abnormalities characterized by fiber atrophy, oxidative stress, mitochondrial dysfunction, impaired Ca^{2+} homeostasis, elevated proteasome dependent proteolysis, but inhibited autophagy/mitophagy, which we speculate offers a novel therapeutic molecular target regulated by a Nox-MuRF1/ubiquitin proteasome-mitochondria-RyR1/Ca^{2+} signaling axis.

Clinical Trial Registration: URL: https://clinicaltrials.gov Unique Identifier: NCT02663115

Keywords: diaphragm; humans; heart failure; MuRF1, NADPH

Non-standard Abbreviations and Acronyms

ATP – adenosine triphosphate
CABG – coronary artery bypass grafting
CHF – chronic heart failure
ETC – electron transfer chain
FEV1 – forced expiratory volume in 1 second
ROS – reactive oxygen species
SR – sarcoplasmic reticulum
UPS – ubiquitin-proteasome system
VC – vital capacity
VE/VCO_2 – ratio ventilation to carbon dioxide output
VO_{2peak} – maximal oxygen uptake

Introduction

The diaphragm is the main respiratory muscle responsible for normal ventilatory behaviors.[1] Diaphragm weakness is common in patients with chronic heart failure (CHF) [2] and is closely associated with symptoms and mortality. [3, 4] Yet, the underlying mechanisms in humans remain only partially resolved [5-8] and most of our knowledge is derived from animal models. [9-11] Of the few human studies performed, most were underpowered, or lacked modern molecular biology approaches [5-8], thus limiting our mechanistic understanding and potential treatment options for the current patient.

Both acute [9] and chronic heart failure [11] cause diaphragm weakness in CHF mouse models, which is characterized by both fiber contractile dysfunction and fiber atrophy. [11-14] Reactive oxygen species (ROS) play a causal role to induce diaphragm weakness [15, 16] since antioxidant interventions such as exercise training [11], pharmacological aids [17], or genetic deletion [18] can prevent diaphragm weakness by reducing posttranslational oxidative modifications of contractile proteins and suppressing protein degradation via the ubiquitin-proteasome system [19] in a MuRF1 dependent manner. [20] In end-stage CHF patients, the diaphragm shows ultra-structural and myofibrillar alterations that implicate metabolic and contractile abnormalities [6, 8], which are related to NADPH signaling. [5] Animal models have identified NADPH oxidase [21] and mitochondria [16, 22] as major sources of ROS, but their role in the human diaphragm remains poorly defined. In addition, the level of structural and molecular alterations in the diaphragm has never been extensively linked to clinical presentation.

We hypothesized that CHF patients would have a distinctive diaphragm myopathy, which would closely correlate to clinical observations. The present study, therefore, evaluated clinical, histological and molecular evidence from diaphragm biopsies in CHF patients scheduled for left ventricular assist device implantation and patients without CHF requiring coronary artery bypass grafting.

Methods

The data that support the findings of this study are available from the corresponding author upon reasonable request. Patients with severe CHF and reduced left ventricular ejection fraction (LV-EF) scheduled for left ventricular assist device implantation and patients with coronary artery disease (control) undergoing elective coronary artery bypass grafting without CHF were eligible for this study. All patients gave written informed consent. The trial was approved by the local ethics committee, complied with the Declaration of Helsinki, and is registered at www.clinicaltrials.gov (Unique Identifier: NCT02663115).

Categorical variables are given as numbers and percentage compared between groups by the chi-squared test or Fisher exact test as appropriate. Continuous variables are shown as mean and 95%-confidence interval irrespective of its distribution assessed by the Shapiro-Wilk-Test. Groups were compared using the Students t-test or Mann-Whitney-U-Test according to normal vs non-normal distribution. Due to limited biopsy size, not all parameters were determined in all biopsies, exact numbers and all values depicted in the *Figures* are given in *Online Table I*. For all the representative images in the manuscript, demonstrative examples reflecting the group mean trend were selected. Correlation analyses were performed using Pearson correlation to evaluate the association of both potential biological pathways predominantly known from animal studies and molecular measures with three defined clinical parameters (diaphragm thickness, VO_{2peak}, VE/VCO_2). A two-sided p-value <0.05 was considered significant.

For detailed methodological information, please refer to the *Online Supplement* and the *Major Resources Table*.

Results

Baseline characteristics

Between January 2016 and December 2017, 18 CHF patients and 21 controls were included. Baseline characteristics are shown in *Table 1*. Compared to controls, CHF were slightly younger, had worse renal function, a lower body mass index, and lower rates of coronary artery disease, but had a higher incidence of atrial fibrillation and previous cardiac surgery (all $p<0.05$). One third of CHF had ischemic and two thirds had dilated cardiomyopathy. With regard to whole body exercise capacity, CHF exhibited a 35% lower VO_{2peak} and a significantly higher VE/VCO_2 slope than controls, whereas the respiratory exchange ratio was comparable indicating physical exhaustion in both groups (*Online Table II*). Catheterization data of CHF are provided in *Online Table III*.

Table 1: Baseline characteristics

	Control n=21	**CHF n=18**	**P-value**
Age [years]	62 (60; 65)	57 (53; 61)	0.014*
Male Gender, n (%)	17 (81.0)	17 (94.4)	0.349†
Caucasian ethnicity, n (%)	21 (100)	18 (100)	n.a.
Body Mass Index [kg/m²]	32.0 (29.5; 34.6)	28.6 (25.9; 31.3)	0.037*
Systolic blood pressure [mmHg]	133 (124; 142)	109 (103; 115)	8.3E-5‡
Heart rate [min^{-1}]	76 (69; 82)	82 (75; 89)	0.180‡
New York Heart Association class			3.4E-4§
I	2 (9.5)	0 (0)	
II	14 (66.7)	2 (11.1)	
III	5 (23.8)	10 (55.6)	
IV	0 (0)	6 (33.3)	
STS-Score (for CABG) [%]	0.42 (0.36; 0.49)	1.58 (1.02; 2.13)	2.3E-7*
Medical history			
Coronary artery disease, n (%)	21 (100)	10 (55.6)	7.1E-4†
Previous Myocardial Infarction, n (%)	1 (4.8)	5 (27.8)	0.077†
Previous percutaneous coronary intervention, n (%)	5 (23.8)	8 (44.4)	0.173§
Previous cardiac surgery, n (%)	0 (0)	4 (22.2)	0.037†
Atrial fibrillation/flutter, n (%)	2 (9.5)	11 (61.1)	6.6E-4§
Arterial hypertension, n (%)	20 (95.2)	17 (94.4)	1.000†
Diabetes mellitus, n (%)	10 (47.6)	10 (55.6)	0.521$
Previous stroke, n (%)	0 (0)	1 (5.6)	0.462†
Peripheral artery disease, n (%)	1 (4.8)	2 (11.1)	0.586†
Chronic kidney disease, stage ≥3b, n (%)	0 (0)	9 (50)	2.3E-4†
Serum creatinine [mmol/l]	78 (71; 84)	122 (100; 144)	1.3E-4‡
Heart failure features			
Ischemic cardiomyopathy, n (%)	n.a.	6 (33.3)	n.a.
Dilated cardiomyopathy, n (%)	n.a.	12 (66.7)	
Number of cardiac decompensation	0 (0; 0)	1.39 (0.93; 1.84	1.1E-7*
NT-proBNP [pg/ml]	244 (84; 405)	3449 (1791; 5108)	1.6E-8*
Echocardiography			
Left ventricular-ejection fraction [%]	61 (58; 64)	19 (17; 22)	8.6E-23‡
Left ventricular enddiastolic diameter [mm]	51 (49; 53)	73 (69; 77)	5.2E-11‡

Left atrial volume index [ml/m²]	34 (28; 41)	63 (54; 72)	6.2E-6*
Right ventricular enddiastolic parameter [mm]	29 (27; 32)	38 (34; 41)	1.4E-4‡
Right atrial area [mm²]	13 (12; 15)	23 (19; 28)	2.8E-4‡
Tricuspid annular plane excursion [mm]	23 (20; 25)	14 (12; 15)	2.6E-7‡
Diameter inferior vena cava [mm]	14 (13; 16)	19 (16; 22)	1.1E-3‡
Lung function			
VC [l]	3.9 (3.4; 4.3)	3.2 (2.9; 3.4)	8.0E-3‡
FEV1 [l]	3.1 (2.8; 3.5)	2.6 (2.3; 2.9)	0.022‡
FEV1/VC [%]	81 (78; 85)	79 (75; 83)	0.250‡
Residual volume [l]	2.7 (2.2; 3.2)	2.5 (2.1; 2.8)	0.466‡
Resistance [kPa/l/s]	0.24 (0.19; 0.29)	0.26 (0.21; 0.32)	0.415*
Transfer coefficient [%]	99 (92; 106)	80 (73; 87)	3.8E-4‡
Treatments at inclusion			
Beta-blocker, n (%)	17 (81.0)	17 (94.4)	0.349†
ACE-inhibitor, n (%)	8 (38.1)	7 (38.9)	0.959§
Angiotensin receptor blocker, n (%)	8 (38.1)	0 (0)	4.0E-3†
Neprylisin inhibitor/angiotensin receptor blocker, n (%)	0 (0)	6 (33.3)	5.7E-3†
Mineral receptor antagonist, n (%)	1 (4.8)	16 (88.9)	1.3E-7§
Digitoxin, n (%)	0 (0)	4 (22.2)	0.037†
Diuretics, n (%)	10 (47.6)	16 (88.9)	6.4E-3§
Intravenous Phosphodiesterase inhibitor, n (%)	0 (0)	15 (83.3)	9.7E-8§
Implantable cardioverter defibrillator, n (%)	0 (0)	16 (88.9)	1.8E-8§
Cardiac resynchronization therapy, n (%)	0 (0)	4 (22.2)	0.037†

Values are expressed as mean with 95%-confidence interval or numbers and percentages. STS indicates Society of Thoracic Surgeons score; CABG, coronary artery bypass grafting; VC, vital capacity; FEV1, forced expiratory volume in 1 second; ACE, angiotensin converting enzyme.
All p-values are two-sided and were not corrected for multiple testing. Continuous variables were tested for normal distribution applying the Shapiro-Wilk-test.
* Mann-Whitney-U-Test
† Fisher exact test
‡ unpaired Students t-test
§ chi-squared test

In vivo respiratory function

Pi_{max} and Pe_{max} were significantly reduced by 38% and 25% in CHF compared to controls (*Figure 1 A*). $P_{0.1}$ was not significantly different between groups; however, $P_{0.1}/Pi_{max}$ ratio was higher in CHF indicating increased ventilatory drive (*Figure 1 B, Online Table II*). Diaphragm wasting was obvious in CHF, with mean diaphragm thickness 23% lower compared to control (*Figure 1 C, Online Table II*). Diaphragm thickness was moderately correlated to Pi_{max} (R=0.44, p=5.0E-3), the latter also correlated to vital capacity (r=0.47; p=3.0E-3) (*Figure 1 D-E*). Spirometry showed vital capacity, absolute FEV_1, and transfer coefficient were lower in CHF, but FEV_1/VC, residual volume und resistance were comparable between groups (*Table 1*). No patient had a FEV1/VC <70% excluding obstructive lung disease.

Diaphragm sampling

No serious adverse events occurred during baseline or diaphragm sampling in either group. The time from intubation to sampling of the diaphragm probes was comparable between both groups (CHF 69 min (95%-CI 53; 85) vs control 64 min (95%-CI 55; 74), p=0.576), which suggests any differences in diaphragm measures were unrelated to mechanical ventilation.

Fiber remodeling

Fiber remodeling involving isoform shift and atrophy are suggested to underpin diaphragm weakness in CHF. We confirmed a fiber-type shift and atrophy in CHF compared to controls: a fast type II to slow type I was observed (p=0.047) alongside atrophy in both type I and type II fibers with lower cross sectional areas of 35% and 51% respectively (*Figure 2 A-D*). The ubiquitin-proteasome system (UPS) is the major proteolytic pathway responsible for protein degradation, which is rate-limited in wasting conditions by upregulation of muscle-specific E3 ligases that include MuRF1 and MAFbx. MuRF1 protein expression was higher by 46% (p=3.9E-4) (*Figure 2 E*), whereas MAFbx protein expression was lower by 35% in CHF vs control (p=2.0E-3) (*Figure 2 F*). However, we assume a higher overall E3 ligase activity in CHF that is supported by a 54% higher protein ubiquitination at lysine 48 residues, with proteasome activity elevated by 54% (p=0.026) (*Figure 2 G-H*). MuRF1 expression was correlated with protein ubiquitination at lysine residues (Ubi-K48) (R=0.46, p=0.017) and Ubi-K48 correlated with proteasome activity (R=0.58, p=2.9E-3) supporting the biological pathway of E3 Ligase dependent proteasome activation. Moreover, MuRF1 protein expression was correlated with clinical parameters (diaphragm thickness (R=-0.46, p=0.015), VO_{2peak} (R=-0.43, p=0.024), VE/VCO_2 (R=0.40, p=0.045)). These data implicate diaphragm weakness and atrophy in CHF is underpinned by MuRF1-dependent ubiquitin-proteasome degradation.

Oxidative stress

Increased oxidative stress leads to 1) activation of UPS components to elevate protein degradation and 2) contractile dysfunction by damaging sarcomeric proteins. [21] As NADPH oxidases are a major source of muscle-derived ROS, we confirmed that protein expression of Nox2 and Nox4 isoforms were 2.8- (p=4.2E-3) and 10.2-fold (p=1.4E-3) higher in CHF vs controls (*Figure 2 I-J*). ROS-induced protein damage was evident in CHF as indicated by a 33% higher carbonylation of myosin heavy chain in CHF vs controls (p=0.015) (*Figure 2 K*), supporting higher oxidation of myofibrillar proteins. Nox2 was correlated to MuRF1 expression (R=0.40, p=0.049) and Ubi-K48 (R=0.67, p<1.0E-4) (*Figure 2 L*). Nox2 also correlated with *in vivo* measures as diaphragm thickness (R=-0.52, p=3.3E-3), VO_{2peak} (R=-0.72, p=1.1E-5) and VE/VCO_2 (R=0.56, p=1.5E-3) (*Online Table IV*). Overall, these data suggest that NADPH oxidases are likely a major upstream mechanism inducing oxidative stress causing diaphragm weakness in human CHF [5], at least partially via 1) activating components of the UPS to elevate protein degradation, leading to muscle atrophy, and 2) inducing contractile dysfunction by damaging sarcomeric proteins. Those molecular mechanisms are linked to whole-body exercise intolerance.

Mitochondrial function and morphology

Since mitochondrial dysfunction is known to play a key role in fiber atrophy, and Nox4 interacts with mitochondria, we next examined the mitochondria. Mitochondria of CHF exhibited a lower citrate synthase activity per mg mitochondrial protein (*Figure 3 A*) and were smaller according to a FACS analysis of all undamaged mitochondria (*Figure 3 B*). In addition, state 3 and state 4 respiration were significantly lower across different substrates for complex I, II, III, and IV in CHF patients compared to controls (*Online Table V*). Respiratory control index and ADP/O ratio were not different between groups irrespective of the substrate indicating comparable phosphorylation efficiency. Representative graphs are shown for palmitoylcarnitine/malate as complex I substrate in *Figure 3 C-F*. State 3 respiration was correlated to *in vivo* measures of ventilatory efficiency (R=-0.58, p=0.012) and diaphragm thickness (r=0.60, p=6.4E-3) (*Figure 3 G-H*) and VO_{2peak} (R=0.57, p=0.014). We used electron microscopy to assess diaphragm mitochondrial morphology in CHF and control samples, which revealed accumulation of intermyofibrillar and subsarcolemmal mitochondria characterized by variable size, but predominately small-sized mitochondria in CHF (*Figure 3 I-L*).

Given that mitochondrial function depends on both intrinsic function and amount, we assessed mitochondrial content in patients by examining different mitochondrial markers and enzyme activities of proteins related to the electron transfer chain (ETC). Mitochondrial quantity was higher in CHF vs controls indicated by a 2.2-fold elevated porin protein expression (*Figure 4 A*) and 1.3-fold higher citrate synthase activity in whole muscle homogenates (*Figure 4 B*). Succinate dehydrogenase activity remained unchanged (*Figure 4 C*). However, after normalizing these values for mitochondrial amount to provide an index of intrinsic mitochondrial function, both ratios for citrate synthase and succinate dehydrogenase activity were significantly lower in CHF (*Figure 4 B-C*). In addition, enzymatic

complex-I activity was reduced by 41% in CHF, which is in line with the reduced complex-I respiration found in isolated mitochondria (*Figure 4 D*). The protein expression of uncoupling protein 3 (UCP3) was higher in CHF compared to controls (p=0.052) (*Figure 4 E*), whereas protein expression of uncoupling protein 2 was not detectable in both CHF and controls (data not shown).
To provide further insights into mitochondrial pathology, we examined parameters of fusion and fission. The protein expression of the fusion parameter Mitofusin-2 (Mfn2) and the fission parameter cytosolic GTPase dynamin-related protein 1 (Drp1) was 2.3-fold (p=1.4E-3) and 1.6-fold (p=0.041) higher in CHF than in controls *(Figure 4 F-G*) suggesting both increased fusion and fission. To assess mitochondria biogenesis, we investigated the protein expression of PGC1alpha found to be 1.5-fold higher in CHF (p=0.032). Autophagy/mitophagy was assessed by evaluating the protein expression of LC3-I/LC3-II and p62. The ratio LC3-I/LC3-II was 1.4-fold higher in CHF (p=9.0E-3) and p62 protein expression was 2-fold higher in CHF (p=1.4E-3). The combination of a reduced lipidation of LC3 and accumulation of p62 indicates inhibited autophagy/mitophagy in CHF. [23]
Overall, these data reveal that despite increased measures of overall number and content, intrinsic dysfunction of mitochondria is present in the CHF diaphragm, potentially caused by impaired mitophagy.

Calcium homeostasis
The observed mitochondrial alterations closely mirror those reported to occur when Ca^{2+} overload is present consequent to "leaky" ryanodine receptor (RyR1). [24] We investigated the binding status of FKBP12 to RyR1, which when reduced is a proxy for "leaky" RyR1 to indicate altered Ca^{2+} homeostasis. Binding of FKBP12 to RyR1 was lower in CHF compared to controls (p=0.050), which indicated Ca^{2+} efflux from the sarcoplasmatic reticulum (SR) into the cytosol (*Figure 5 A*). There was a parallel significant increase in protein expression of Ca^{2+} re-uptake proteins in CHF including SERCA-1 and SERCA-2A (*Figure 5 B-C*). Elevated Ca^{2+} levels can also activate Ca^{2+}-dependent proteases such as calpains to promote fiber atrophy. [25] We therefore measured calpain activity but did not find a significant difference between groups (*Figure 5 D*), which suggests that catabolic activity in the diaphragm of humans with CHF is potentially driven by the UPS. Impaired Ca^{2+} homeostasis can also limit excitation-contraction coupling to impair diaphragm contractile function and induce weakness. As such, we next assessed Ca^{2+}-activated single-fiber contractile function in isolated diaphragm type II fibers, which revealed significantly reduced myofilament Ca^{2+} sensitivity in CHF vs controls (*Figure 5 E-F*).

Discussion

Our data show that CHF patients suffer from a diaphragm myopathy that occurs independent of disuse or other confounding factors such as ageing, obesity, or hypertension. Specifically, we confirm using *in vivo* and *in vitro* approaches that diaphragm weakness and wasting is present in CHF, which is underpinned by severe cellular remodeling and molecular alterations that include fiber atrophy, NOX-related oxidative stress, proteasome-linked catabolic activation, mitochondrial dysfunction, and impaired Ca^{2+} homeostasis. Clinically, the molecular alterations closely correlate to both whole-body exercise capacity and respiratory function. Thus our data reveal, for the first time in humans with heart failure, a novel molecular mechanism and potential therapeutic target for diaphragm weakness that is centered around a Nox-MuRF1/ubiquitin proteasome-mitochondria-RyR1/Ca^{2+} dependent signaling axis.

Patient population and clinical data

The CHF group comprised patients with exercise capacity reduced to 57% of the age- and sex-specific predicted norm. CPX was performed in part under inotropic support, which might explain the slightly higher VO_{2peak} compared to other left ventricular assist device studies. [26, 27] In the control group, we included non-CHF patients undergoing elective coronary artery bypass grafting. Clinically, control patients did not have CHF and presented with normal measures of LV-EF, nt-proBNP and VO_{2peak}. Moreover, we excluded patients in both groups with comorbidities known to influence the morphology and function of the diaphragm, in particular recent mechanical ventilation, COPD, severe chronic and/or acute renal failure.

The magnitude of diaphragm dysfunction in our study was comparable to other studies including those examining Pi_{max} as a prognostic marker [3, 4] and including NYHA III/IV patients who have pronounced diaphragm weakness. [28] The ratio $P_{0.1}/Pi_{max}$, commonly interpreted as an index for ventilatory drive, was higher in CHF compared to controls and comparable to published data. [28] This observation is consistent with rapid shallow breathing commonly found in advanced CHF. Despite this increased workload, we found reduced diaphragm thickness in CHF, which is an index of atrophy closely associated with exercise intolerance in CHF. [29] Structural changes in CHF were associated with *in vivo* respiratory dysfunction and cellular markers of proteolysis (i.e. MuRF1) and mitochondrial derangements.

NADPH oxidase as a major mechanism triggering diaphragm weakness

NADPH oxidases have emerged as one major source of ROS in skeletal muscle cells. [21] An increased NADPH expression has been observed in both acute [9] and chronic animal models of heart failure. [18] Increased Nox2 protein expression in the diaphragm of CHF patients is in line with a former study examining Nox2 and its downstream mediators. [5] An ~40% increase of ROS induced protein damage was also evident [5], which is similar to the increased carbonylation of MHC in our study.

ROS, but also cytokines, angiotensin II and sphingomyelinase, are able to activate proteolytic pathways in skeletal muscle including the UPS. [30] In the diaphragm of CHF, the UPS appeared to be the dominant proteolytic system since calpain activity was not significantly different between groups. Moreover, Nox2 and Nox 4 protein expression was correlated to activation of the key atrogene, muscle-specific E3 ligase MuRF1, and protein ubiquitination, thus supporting the biological pathway of MuRF1-dependent proteasome degradation of proteins. Both Nox2 and the UPS are linked to diaphragm weakness in animal models [18, 31] and the genetic knock out of the p47(phox)-Nox2 subunit is associated with reduced ROS production and preservation of diaphragm function. [18] In humans, the correlation of Nox2 and MuRF1 to *in vivo* measures of diaphragm morphology and function supports the association between increased ROS/catabolic activity and whole-body symptoms related to exercise intolerance and respiratory dysfunction. While we saw an increase in MuRF1 expression, MAFbx was lower in CHF than in controls. This phenomenon has been observed before with unchanged or reduced expression levels in humans and animals with heart failure and/or after exercise training. [10, 32, 33] However, we assume a higher overall E3 ligase activity in CHF supported by increased polyubiquitination at lysine 48 residues and proteasome activity in CHF, with the former one being the typical polyubiquitination signal for proteasome dependent degradation [34]. Reduction of MAFbx, which predominantly leads to degradation of initiation factor 3 subunit 5 (eIF3-f) and MyoD[35], might be a compensation to the increased proteolysis of structural proteins by MuRF1 since an increase in eIF3-f leads to increased expression of

structural proteins and causes muscle hypertrophy. [36] Further research is necessary to investigate the interaction between these two E3 ligases.

Many studies have focused on Nox2, however, the role of Nox4 in skeletal muscle and the diaphragm of CHF patients is not well defined. While Nox2 is regulated by phosphorylation of p47(phox) or p67(phox), and activation of Rac1, Nox4 is constitutively active and, therefore, transcriptionally regulated. [21] We found an astonishing 10.2-fold higher Nox4 protein expression in the diaphragm of CHF indicating increased Nox4 activity. While Nox2 is a sarcolemmal protein, Nox4 contains a mitochondria localization sequence in its N-terminal region and is found in muscle mitochondria and sarcoplasmic reticulum (SR). [21] Therefore, we assessed mitochondrial function and parameters of calcium handling to provide further mechanistic insight.

Mitochondrial function and calcium handling

In isolated mitochondria, we found reduced state 3 and state 4 respiration across different substrates for complex I-IV in CHF. Electron microscopy revealed accumulation of intermyofibrillar and subsarcolemmal mitochondria in CHF characterized by variable size, but predominately small-sized mitochondria, which is in line with the results of the FACS analysis of isolated mitochondria. This might be the consequence of inhibited autophagy/mitophagy with an imbalance between fusion and fission, which is discussed below. Increased markers of mitochondria quantity (citrate synthase, porin) supported a higher amount of mitochondria in CHF. The reduced respiratory capacity across all four electron transport chain (ETC) complexes suggests a defect in complex IV and/or assembly of supercomplexes. [37] However, this does not exclude impairments in other complex activities. Indeed, we proved a reduction in enzymatic complex-I- and succinate dehydrogenase activity suggesting that reduced respiration of complex I and II is not only due to a defect in complex IV but also caused by complex specific alterations. This may finally lead to a reduced proton gradient across the inner membrane with reduced capacity for ATP production contributing to impaired muscle function and exercise capacity. [38] From a clinical point of view, this hypothesis is supported by our correlative analysis between a reduced state 3 respiration vs ventilatory efficiency and VO_{2peak} derived from whole body exercise testing.

To elucidate potential reasons for the impaired mitochondrial function in CHF, we evaluated markers controlling the quality of the mitochondrial network. A higher protein expression of Mfn2 and Drp1 in CHF indicates increased fusion and fission. Both parameters are sensitive to exercise [39] and the observed higher expression might be the consequence of a higher ventilatory workload in CHF. The same could be the case for PGC1alpha known to be very sensitive to exercise. [39] In contrast, the combination of a reduced lipidation of LC3 and accumulation of p62 indicates inhibition of autophagy/mitophagy in CHF. [23] Blocked mitophagy is associated with a diminished mitochondrial function [40] and protein expression of ETC enzymes. [39] Therefore, this finding might serve as an explanation for the reduced mitochondrial function observed in the diaphragm of CHF patients. Further research is necessary to elucidate the reasons for autophagy inhibition.

Moreover, we found an increased UCP3 expression, which can be the consequence of elevated ROS. Increased UCP3 is found after acute exercise and is thought to alleviate the proton gradient across the inner membrane, thereby reducing excessive ROS production but also ATP production by the ETC. [41] In CHF, a similar scenario may occur in response to the increased work of breathing and acute episodes of dyspnea [7], potentially aggravated by hypoxia. [42] Another hypothesis is Nox4 induced mitochondrial stress, which is supported by the correlation between Nox4 and UCP3 in our patient cohort. Cardiac-specific Nox4-deletion attenuated mitochondrial dysfunction in response to pressure overload in mice being associated with reduced ROS production and oxidative damage to mitochondrial proteins. [43]

Several mechanisms can account for the cross talk between Nox4, mitochondria and the SR including oxidation of mitochondrial ETC proteins or oxidation of the RyR within the SR. [21] The latter one causes a Ca^{2+} leak from the SR. [24] Mitochondria act as a buffer with the result of Ca^{2+} overload, which in return induces mitochondrial dysfunction. [24] Additionally, impaired mitophagy is associated with increased mitochondrial Ca^{2+} uptake and a reduced Ca^{2+} availability for contraction. [40] Such a feedback-loop between the SR and mitochondria in which SR Ca^{2+} leak triggers mitochondrial dysfunction has been described in failing myocytes [24] and in the diaphragm during mechanical ventilation. [44] Against this background, we examined the binding status of the subunit FKBP12 to RyR1, which if reduced is a molecular marker of a “leaky” receptor state. Binding of FKBP12 to RyR1 was lower in CHF compared

to controls suggesting increased Ca^{2+} efflux from the SR. We also found an increased protein expression of calcium re-uptake handling proteins in CHF, which likely indicates a compensatory response to elevated Ca^{2+} levels by increasing reuptake pumping. Moreover, single-fiber contractile function from CHF patients was impaired, showing reduced Ca^{2+} sensitivity. The rightward shift of the pCa^{2+}-force curve indicates that diaphragm fibers of CHF patients generate a lower force of their maximal for a given Ca^{2+} concentration. [14] This suggests that contractile function in the CHF diaphragm is even more affected at submaximal than at maximal activation, which is clinically relevant as the diaphragm most often works at submaximal workloads. Overall, our data confirm impaired Ca^{2+} homeostasis in the diaphragm of CHF patients, which is caused by leaky RyR1 coupled to reduced myofibrillar sensitivity and mitochondrial dysfunction.

Limitations

Our results should be interpreted against the background of the following limitations. First, the control group was not a healthy comparator since patients had coronary artery disease requiring coronary artery bypass grafting; however, for reasons of gathering both clinical data and diaphragm biopsy, this was the most appropriate group in our setting. Second, CHF were slightly younger than controls. We believe that the difference of 7 years was not clinically meaningful. It even underlines the robustness of our findings since respiratory function decreases with age. Third, CHF comprised both ischemic and dilated cardiomyopathy, but number of patients was not sufficient to make meaningful comparisons between both entities. Fourth, Nox2 and Nox4 subunits are expressed in several other cell types (e.g., macrophages, endothelium, and smooth muscle cells), which may have made minor contribution to our muscle homogenate data. Fifth, single fiber measurement could only be done in type II fibers due to contracted type I fibers. Preserving techniques are well established for those contractile measurements [45, 46]; therefore, this phenomenon remains unclear. However, we do not believe that it was a disease specific problem because it was found in both CHF and control probes. Moreover, we cannot rule out that a fiber selection bias affected the outcomes of our contractility assays. To minimize this effect, we randomly selected fibers for the contractile assays and excluded only those exhibiting injury patterns that are associated with impossible or unreliable single fiber measurement. Sixth, our data are descriptive and despite correlative evidence, we cannot provide a cause-relationship despite our assumptions being supported in some instances by genetic knock out models. We were also not able to examine all the downstream mediators known to be responsible for ROS production by NADPH oxidases due to tissue limitation. [21] Moreover, we are not able to distinguish between causative and compensatory molecular events since it is a single time point analysis in humans and correlation analysis does not mean causality. To elucidate cause and compensation, longitudinal experiments with specific therapies aimed at specific molecular components would be necessary. However, it is important to recognize that the pathophysiology of diaphragm dysfunction seen in different animal models (e.g. catabolic activation, mitochondrial dysfunction, Nox activation) is also present in human specimens. Those results form a solid base for development and testing of different treatment strategies in CHF to address respiratory and skeletal muscle dysfunction including MuRF1 inhibition [47, 48], increasing Ca^{2+} sensitivity [49] or Nox inhibition. [50]

Conclusions

CHF patients demonstrate a diaphragm myopathy independent of disuse or other confounding factors such as ageing, obesity, or hypertension. *In vivo* diaphragm weakness and wasting induced by CHF were associated with intracellular abnormalities characterized by fiber atrophy, oxidative stress, mitochondrial dysfunction, impaired Ca^{2+} homeostasis, elevated proteasome dependent proteolysis, but inhibited autophagy/mitophagy, which we speculate is regulated via a Nox-MuRF1/ubiquitin proteasome-mitochondria-RyR1/Ca^{2+} signaling axis to offer a novel therapeutic molecular target (*Figure 6*).

Acknowledgement
We are grateful to Claire Boulogne and Cynthia Gillet as the present work has benefited from Imagerie-Gif core facility supported by l'Agence Nationale de la Recherche (ANR-11-EQPX-0029/Morphoscope, ANR-10-INBS-04/FranceBioImaging; ANR-11-IDEX-0003-02/ Saclay Plant Sciences).

Funding
NM received funding from the Leipzig Heart Institute (HRC060453). TSB received funding from the Medical Research Council UK (MR/S025472/1) and Heart Research UK (TRP 16/19).

Disclosures

Norman Mangner reports personal fees from Edwards LifeScience, Medtronic, Biotronik, Novartis, Sanofi Genzyme, Bayer, Pfizer, and AstraZeneca, outside the submitted work.
Jens Garbade has nothing to disclose.
Estelle Heyne has nothing to disclose.
Marloes van den Berg has nothing to disclose.
Ephraim B. Winzer reports personal fees from Boehringer-Ingelheim, CVRx, and Novartis, outside the submitted work.
Jennifer Hommel has nothing to disclose.
Marcus Sandri has nothing to disclose.
Joanna Jozwiak-Nozdrzykowska has nothing to disclose.
Anna L. Meyer has nothing to disclose.
Sven Lehmann has nothing to disclose.
Clara Schmitz has nothing to disclose.
Edoardo Malfatti has nothing to disclose.
Michael Schwarzer has nothing to disclose.
Coen A. C. Ottenheijm has nothing to disclose.
T. Scott Bowen has nothing to disclose.
Axel Linke reports grants from Novartis, personal fees from Medtronic, Abbott, Edwards Lifesciences, Boston Scientific, Astra Zeneca, Novartis, Pfizer, Abiomed, Bayer, Boehringer, and other from Picardia, Transverse Medical, Claret Medical, outside the submitted work.
Volker Adams has nothing to disclose.

Supplemental Materials

Expanded Materials & Methods

Online Tables I - V

References only in the Supplement [51-61]

Figure Legend

Figure 1 – Clinical assessment of respiratory function. Reduced inspiratory (Pi_{max}) and expiratory function (Pe_{max}) in patients with heart failure (CHF) compared to control patients (A). $P_{0.1}$ was equal between groups, but the ratio $P_{0.1}/Pi_{max}$ was higher in CHF indicating increased respiratory drive (B). Diaphragm thickness was lower in CHF for both right and left hemi-diaphragm (C). Reduced diaphragm thickness was associated with reduced Pi_{max} (D). Pi_{max} was associated with reduced vital capacity (E).
Number of patients: A-D) control: 21, CHF: 18; E) control: 20, CHF: 17.
All p-values are two-sided and were not corrected for multiple testing.
Continuous variables were tested for normal distribution applying the Shapiro-Wilk-test.
* unpaired Students t-test.
† Mann-Whitney-U-Test.

Figure 2 – Diaphragm fiber phenotype, ubiquitin-proteasome system, and NADPH oxidase. Immunostaining of type-1 fibers (brown) in the diaphragm of control (A) and CHF (B). In seven control and six CHF patients, an average of 288 type-1 and 164 type-2 fibers per patient were analyzed; statistical comparisons were made between control and CHF for each fiber type regarding distribution and cross-sectional area (CSA). CHF had a shift towards type-1 fibers (C) with a reduction of CSA in both type-1 (slow) and type-2 (fast) fibers (D). Protein expression of the muscle-specific E3-ligase MuRF1 (E) was higher, whereas the protein expression of another E3-ligase MafBx (F) was lower in CHF vs controls. Protein ubiquitination (G) and proteasome activity (H) were higher in CHF vs controls. Protein expression of the NADPH oxidase isoforms Nox2 (I) and Nox4 (J) were higher in CHF vs controls. The amount of carbonylated myosin heavy chain (MHC) was higher in CHF vs controls (J). Nox2 protein expression was correlated to protein ubiquitination (K).
Number of patients: E) control: 16, CHF: 11; F) control: 19, CHF: 12; G) control: 18, CHF: 12; H) control: 16, CHF: 9; I) control: 18, CHF: 12; J) control: 15, CHF: 12; K) control: 6, CHF: 6; L) control: 16, CHF: 11.
All p-values are two-sided and were not corrected for multiple testing.
Continuous variables were tested for normal distribution applying the Shapiro-Wilk-test.
* unpaired Students t-test.
† Mann-Whitney-U-Test.

Figure 3 – Isolated mitochondrial measures. The activity of citrate synthase (relative to mitochondrial protein content) (A) and mitochondrial size (B) was lower in CHF vs controls. State 3 (C) and state 4 respiration (D) of complex I using palmitoylcarnitine/malate as substrate with significantly lower values in CHF vs controls. The respiratory control index (RCI, E) and ADP/O ratio (F) were comparable between both groups. State 3 respiration (glutamate/malate) was associated with exercise capacity (G) and diaphragm thickness (H). Electron micrograph showing normal mitochondria localized in correspondence of sarcomeric Z-disk in a control patient (I, J). In CHF, we found intermyofibrillar mitochondria with small size (K) and prominent accumulation of mitochondria with variable size in subsarcolemmal areas (L).
Number of patients: A) control: 12, CHF: 9; B) control: 10, CHF: 5; C) control: 11, CHF: 6; D) control: 11, CHF: 6; E) control: 11, CHF: 6; F) control: 11, CHF: 6; G) control: 12, CHF: 6; H) control: 12, CHF: 6; I-L) control: 5, CHF: 5.
All p-values are two-sided and were not corrected for multiple testing.
Continuous variables were tested for normal distribution applying the Shapiro-Wilk-test.
* unpaired Students t-test.
† Mann-Whitney-U-Test.

Figure 4 – Mitochondrial protein, enzyme activities and morphology. Protein expression of porin (A) and citrate synthase activity (B, left side) was higher in CHF vs controls indicating increased mitochondrial content. Citrate synthase activity relative to porin expression (B, right side) and succinate dehydrogenase activity relative to porin expression (C, right side) were lower in CHF vs controls, whereas absolute succinate dehydrogenase activity was not different (C, left side). Enzymatic complex I activity was significantly lower in CHF vs controls (D). Protein expression of uncoupling protein 3

(UCP3) was higher in CHF (E). Higher protein expression of Mfn2 (F) and Drp1 (G) in CHF vs controls. Protein expression of PGC1alpha was higher in CHF vs controls (H). Both LC3-I/LC3-II ratio (I) and p62 protein expression (J) were higher in CHF vs controls.
Number of patients: A) control: 16, CHF: 12; B) control: 17/15, CHF: 9; C) control: 16, CHF: 12; D) control: 14, CHF: 9; E) control: 17, CHF: 12; F) control: 17, CHF: 11; G) control: 15, CHF: 12; H) control: 19, CHF: 12; I) control: 16, CHF: 12; J) control: 17, CHF: 11.
All p-values are two-sided and were not corrected for multiple testing.
Continuous variables were tested for normal distribution applying the Shapiro-Wilk-test.
* unpaired Students t-test.
† Mann-Whitney-U-Test.

Figure 5 – Markers of calcium homeostasis in the diaphragm. Immunoprecipitation for RyR1 showing reduced binding of FKBP12 in CHF vs controls (A). Protein expression of SERCA-1 (B) and SERCA-2A (C) were higher in CHF vs controls. Calpain activity was not different between CHF and controls (D). Calcium sensitivity was lower in CHF when measured in isolated single type II fibers (E-F).
Number of patients: A) control: 4, CHF: 4; B) control: 17, CHF: 13; C) control: 18, CHF: 11; D) control: 14, CHF: 9; E-F) control: 12, CHF: 9 (an average of 12 fibers per subject were evaluated).
All p-values are two-sided and were not corrected for multiple testing.
Continuous variables were tested for normal distribution applying the Shapiro-Wilk-test.
* unpaired Students t-test.
† Mann-Whitney-U-Test.

Figure 6 – Proposed mechanisms in Heart Failure associated Diaphragm Dysfunction (HFaDD) based on the presented data. Sarcolemmal-bound Nox2 and sarcoplasmic reticulum (SR) and mitochondrial associated Nox4 are two major sources of reactive oxygen species (ROS) that drive diaphragm weakness via promoting fiber atrophy and contractile dysfunction. ROS-mediated activation of the ubiquitin-proteasome system (UPS) to induce atrophy in a MuRF1-dependent manner, while also inducing protein oxidation to impair key contractile proteins such as myosin heavy chain. Inhibited mitophagy, ROS-mediated mitochondrial dysfunction and damage of the SR to induce calcium efflux via “leaky” ryanodine receptors, which proceeds as a vicious circle to exacerbate mitochondrial and contractile dysfunction.

Reference List

(1) **Sieck GC, Fournier M. Diaphragm motor unit recruitment during ventilatory and nonventilatory behaviors.** ***J Appl Physiol (1985).*** **1989;66:2539-45**

(2) **Frankenstein L, Nelles M, Meyer FJ, Sigg C, Schellberg D, Remppis BA, Katus HA, Zugck C. Validity, prognostic value and optimal cutoff of respiratory muscle strength in patients with chronic heart failure changes with beta-blocker treatment.** ***Eur J Cardiovasc Prev Rehabil.*** **2009;16:424-9**

(3) **Meyer FJ, Borst MM, Zugck C, Kirschke A, Schellberg D, Kubler W, Haass M. Respiratory Muscle Dysfunction in Congestive Heart Failure: Clinical Correlation and Prognostic Significance.** ***Circulation.*** **2001;103:2153-8**

(4) **Ribeiro JP, Chiappa GR, Neder JA, Frankenstein L. Respiratory muscle function and exercise intolerance in heart failure.** ***Curr Heart Fail Rep.*** **2009;6:95-101**

(5) **Ahn B, Coblentz PD, Beharry AW, Patel N, Judge AR, Moylan JS, Hoopes CW, Bonnell MR, Ferreira LF. Diaphragm Abnormalities in Patients with End-Stage Heart Failure: NADPH Oxidase Upregulation and Protein Oxidation.** ***Front Physiol.*** **2016;7:686**

(6) **Lindsay DC, Lovegrove CA, Dunn MJ, Bennett JG, Pepper JR, Yacoub MH, Poole-Wilson PA. Histological abnormalities of muscle from limb, thorax and diaphragm in chronic heart failure.** ***Eur Heart J.*** **1996;17:1239-50**

(7) **Tikunov B, Levine S, Mancini D. Chronic congestive heart failure elicts adaptations of endurance exercise in diaphragmatic muscle.** ***Circulation.*** **1997;95:910-6**

(8) **Tikunov BA, Mancini D, Levine S. Changes in myofibrillar protein composition of human diaphragm elicited by congestive heart failure.** ***J Mol Cell Cardiol.*** **1996;28:2537-41**

(9) **Bowen TS, Mangner N, Werner S, Glaser S, Kullnick Y, Schrepper A, Doenst T, Oberbach A, Linke A, Steil L, et al. Diaphragm muscle weakness in mice is early-onset post myocardial infarction and associated with elevated protein oxidation.** ***J Appl Physiol (1985).*** **2015;118:11-9**

(10) **Mangner N, Weikert B, Bowen TS, Sandri M, Hollriegel R, Erbs S, Hambrecht R, Schuler G, Linke A, Gielen S, et al. Skeletal muscle alterations in chronic heart failure: differential effects on quadriceps and diaphragm.** ***J Cachexia Sarcopenia Muscle.*** **2015;6:381-90**

(11) **Mangner N, Bowen TS, Werner S, Fischer T, Kullnick Y, Oberbach A, Linke A, Steil L, Schuler G, Adams V. Exercise Training Prevents Diaphragm Contractile Dysfunction in Heart Failure.** ***Med Sci Sports Exerc.*** **2016;48:2118-24**

(12) **Howell S, Maarek JM, Fournier M, Sullivan K, Zhan WZ, Sieck GC. Congestive heart failure: differential adaptation of the diaphragm and latissimus dorsi.** ***J Appl Physiol (1985).*** **1995;79:389-97**

(13) **Stassijns G, Gayan-Ramirez G, De LP, de B, V, Dom R, Lysens R, Decramer M. Effects of dilated cardiomyopathy on the diaphragm in the Syrian hamster.** ***Eur Respir J.*** **1999;13:391-7**

(14) **van Hees HWH, van der Heijden HFM, Ottenheijm CAC, Heunks LMA, Pigmans CJC, Verheugt FWA, Brouwer RMHJ, Dekhuijzen PNR. Diaphragm single-fiber weakness and**

loss of myosin in congestive heart failure rats. *Am J Physiol Heart Circ Physiol.* 2007;293:H819-H828

(15) Mangner N, Linke A, Oberbach A, Kullnick Y, Gielen S, Sandri M, Hoellriegel R, Matsumoto Y, Schuler G, Adams V. Exercise training prevents TNF-alpha induced loss of force in the diaphragm of mice. *PLoS One.* 2013;8:e52274

(16) Supinski GS, Callahan LA. Diaphragmatic free radical generation increases in an animal model of heart failure. *J Appl Physiol (1985).* 2005;99:1078-84

(17) Hardin BJ, Campbell KS, Smith JD, Arbogast S, Smith JL, Moylan JS, Reid MB. TNF-a acts via TNFR1 and muscle-derived oxidants to depress myofibrillar force in murine skeletal muscle. *J Appl Physiol.* 2008;104:694-9

(18) Ahn B, Beharry AW, Frye GS, Judge AR, Ferreira LF. NAD(P)H oxidase subunit p47phox is elevated, and p47phox knockout prevents diaphragm contractile dysfunction in heart failure. *Am J Physiol Lung Cell Mol Physiol.* 2015;309:L497-L505

(19) van Hees HWH, Li YP, Ottenheijm CAC, Jin B, Pigmans CJC, Linkels M, Dekhuijzen PNR, Heunks LMA. Proteasome inhibition improves diaphragm function in congestive heart failure rats. *Am J Physiol Lung Cell Mol Physiol.* 2008;294:L1260-L1268

(20) Nguyen T, Bowen TS, Augstein A, Schauer A, Gasch A, Linke A, Labeit S, Adams V. Expression of MuRF1 or MuRF2 is essential for the induction of skeletal muscle atrophy and dysfunction in a murine pulmonary hypertension model. *Skelet Muscle.* 2020;10:12

(21) Ferreira LF, Laitano O. Regulation of NADPH oxidases in skeletal muscle. *Free Radic Biol Med.* 2016;98:18-28

(22) Laitano O, Ahn B, Patel N, Coblentz PD, Smuder AJ, Yoo JK, Christou DD, Adhihetty PJ, Ferreira LF. Pharmacological targeting of mitochondrial reactive oxygen species counteracts diaphragm weakness in chronic heart failure. *J Appl Physiol (1985).* 2016;120:733-42

(23) Masiero E, Agatea L, Mammucari C, Blaauw B, Loro E, Komatsu M, Metzger D, Reggiani C, Schiaffino S, Sandri M. Autophagy is required to maintain muscle mass. *Cell Metab.* 2009;10:507-15

(24) Santulli G, Xie W, Reiken SR, Marks AR. Mitochondrial calcium overload is a key determinant in heart failure. *Proc Natl Acad Sci U S A.* 2015;112:11389-94

(25) Bellinger AM, Mongillo M, Marks AR. Stressed out: the skeletal muscle ryanodine receptor as a target of stress. *J Clin Invest.* 2008;118:445-53

(26) Dunlay SM, Allison TG, Pereira NL. Changes in cardiopulmonary exercise testing parameters following continuous flow left ventricular assist device implantation and heart transplantation. *J Card Fail.* 2014;20:548-54

(27) Rosenbaum AN, Dunlay SM, Pereira NL, Allison TG, Maltais S, Stulak JM, Joyce LD, Kushwaha SS. Determinants of Improvement in Cardiopulmonary Exercise Testing After Left Ventricular Assist Device Implantation. *ASAIO J.* 2018;64:610-5

(28) Filusch A, Ewert R, Altesellmeier M, Zugck C, Hetzer R, Borst MM, Katus HA, Meyer FJ. Respiratory muscle dysfunction in congestive heart failure-the role of pulmonary hypertension. *Int J Cardiol.* 2011;150:182-5

(29) **Miyagi M, Kinugasa Y, Sota T, Yamada K, Ishisugi T, Hirai M, Yanagihara K, Haruki N, Matsubara K, Kato M, et al. Diaphragm Muscle Dysfunction in Patients With Heart Failure.** ***J Card Fail.*** **2018;24:209-16**

(30) **Kelley RC, Ferreira LF. Diaphragm abnormalities in heart failure and aging: mechanisms and integration of cardiovascular and respiratory pathophysiology.** ***Heart Fail Rev.*** **2017;22:191-207**

(31) **Adams V, Mangner N, Gasch A, Krohne C, Gielen S, Hirner S, Thierse HJ, Witt CC, Linke A, Schuler G, et al. Induction of MuRF1 Is essential for TNF-alpha induced loss of muscle function in mice.** ***J Mol Biol.*** **2008;384:48-59**

(32) **Gielen S, Sandri M, Kozarez I, Kratzsch J, Teupser D, Thiery J, Erbs S, Mangner N, Lenk K, Hambrecht R, et al. Exercise training attenuates MuRF-1 expression in the skeletal muscle of patients with chronic heart failure independent of age: the randomized Leipzig Exercise Intervention in Chronic Heart Failure and Aging catabolism study.** ***Circulation.*** **2012;125:2716-27**

(33) **Hollriegel R, Beck EB, Linke A, Adams V, Mobius-Winkler S, Mangner N, Sandri M, Gielen S, Gutberlet M, Hambrecht R, et al. Anabolic effects of exercise training in patients with advanced chronic heart failure (NYHA IIIb): impact on ubiquitin-protein ligases expression and skeletal muscle size.** ***Int J Cardiol.*** **2013;167:975-80**

(34) **Vainshtein A, Sandri M. Signaling Pathways That Control Muscle Mass.** ***Int J Mol Sci.*** **2020;21:4759**

(35) **Foletta VC, White LJ, Larsen AE, Leger B, Russell AP. The role and regulation of MAFbx/atrogin-1 and MuRF1 in skeletal muscle atrophy.** ***Pflugers Arch.*** **2011;461:325-35**

(36) **Lagirand-Cantaloube J, Offner N, Csibi A, Leibovitch MP, Batonnet-Pichon S, Tintignac LA, Segura CT, Leibovitch SA. The initiation factor eIF3-f is a major target for atrogin1/MAFbx function in skeletal muscle atrophy.** ***EMBO J.*** **2008;27:1266-76**

(37) **Brand MD, Nicholls DG. Assessing mitochondrial dysfunction in cells.** ***Biochem J.*** **2011;435:297-312**

(38) **Osterholt M, Nguyen TD, Schwarzer M, Doenst T. Alterations in mitochondrial function in cardiac hypertrophy and heart failure.** ***Heart Fail Rev.*** **2013;18:645-56**

(39) **Ju JS, Jeon SI, Park JY, Lee JY, Lee SC, Cho KJ, Jeong JM. Autophagy plays a role in skeletal muscle mitochondrial biogenesis in an endurance exercise-trained condition.** ***J Physiol Sci.*** **2016;66:417-30**

(40) **Favaro G, Romanello V, Varanita T, Andrea DM, Morbidoni V, Tezze C, Albiero M, Canato M, Gherardi G, De SD, et al. DRP1-mediated mitochondrial shape controls calcium homeostasis and muscle mass.** ***Nat Commun.*** **2019;10:2576**

(41) **Jiang N, Zhang G, Bo H, Qu J, Ma G, Cao D, Wen L, Liu S, Ji LL, Zhang Y. Upregulation of uncoupling protein-3 in skeletal muscle during exercise: a potential antioxidant function.** ***Free Radic Biol Med.*** **2009;46:138-45**

(42) **O'Leary AJ, O'Halloran KD. Diaphragm muscle weakness and increased UCP-3 gene expression following acute hypoxic stress in the mouse.** ***Respir Physiol Neurobiol.*** **2016;226:76-80**

(43) **Kuroda J, Ago T, Matsushima S, Zhai P, Schneider MD, Sadoshima J. NADPH oxidase 4 (Nox4) is a major source of oxidative stress in the failing heart.** ***Proc Natl Acad Sci U S A.*** **2010;107:15565-70**

(44) **Matecki S, Dridi H, Jung B, Saint N, Reiken SR, Scheuermann V, Mrozek S, Santulli G, Umanskaya A, Petrof BJ, et al. Leaky ryanodine receptors contribute to diaphragmatic weakness during mechanical ventilation.** ***Proc Natl Acad Sci USA.*** **2016;113:9069-74**

(45) **Hooijman PE, Beishuizen A, Witt CC, de Waard MC, Girbes AR, Spoelstra-de Man AM, Niessen HW, Manders E, van Hees HW, van den Brom CE, et al. Diaphragm Muscle Fiber Weakness and Ubiquitin-Proteasome Activation in Critically Ill Patients.** ***Am J Respir Crit Care Med.*** **2015;191:1126-38**

(46) **van den Berg M, Hooijman PE, Beishuizen A, de Waard MC, Paul MA, Hartemink KJ, van Hees HWH, Lawlor MW, Brocca L, Bottinelli R, et al. Diaphragm Atrophy and Weakness in the Absence of Mitochondrial Dysfunction in the Critically Ill.** ***Am J Respir Crit Care Med.*** **2017;196:1544-58**

(47) **Adams V, Bowen TS, Werner S, Barthel P, Amberger C, Konzer A, Graumann J, Sehr P, Lewis J, Provaznik J, et al. Small-molecule-mediated chemical knock-down of MuRF1/MuRF2 and attenuation of diaphragm dysfunction in chronic heart failure.** ***J Cachexia Sarcopenia Muscle.*** **2019;10:1102-15**

(48) **Bowen TS, Adams V, Werner S, Fischer T, Vinke P, Brogger MN, Mangner N, Linke A, Sehr P, Lewis J, et al. Small-molecule inhibition of MuRF1 attenuates skeletal muscle atrophy and dysfunction in cardiac cachexia.** ***J Cachexia Sarcopenia Muscle.*** **2017;8:939-53**

(49) **Hwee DT, Kennedy AR, Hartman JJ, Ryans J, Durham N, Malik FI, Jasper JR. The small-molecule fast skeletal troponin activator, CK-2127107, improves exercise tolerance in a rat model of heart failure.** ***J Pharmacol Exp Ther.*** **2015;353:159-68**

(50) **Altenhofer S, Radermacher KA, Kleikers PW, Wingler K, Schmidt HH. Evolution of NADPH Oxidase Inhibitors: Selectivity and Mechanisms for Target Engagement.** ***Antioxid Redox Signal.*** **2015;23:406-27**

(51) **Bowen TS, Rolim NP, Fischer T, Baekkerud FH, Medeiros A, Werner S, Bronstad E, Rognmo O, Mangner N, Linke A, et al. Heart failure with preserved ejection fraction induces molecular, mitochondrial, histological, and functional alterations in rat respiratory and limb skeletal muscle.** ***Eur J Heart Fail.*** **2015;17:263-72**

(52) **Chance B, WILLIAMS GR. Respiratory enzymes in oxidative phosphorylation. III. The steady state.** ***J Biol Chem.*** **1955;217:409-27**

(53) **Dabkowski ER, Williamson CL, Bukowski VC, Chapman RS, Leonard SS, Peer CJ, Callery PS, Hollander JM. Diabetic cardiomyopathy-associated dysfunction in spatially distinct mitochondrial subpopulations.** ***Am J Physiol Heart Circ Physiol.*** **2009;296:H359-H369**

(54) **Dzeja PP, Pucar D, Redfield MM, Burnett JC, Terzic A. Reduced activity of enzymes coupling ATP-generating with ATP-consuming processes in the failing myocardium.** ***Mol Cell Biochem.*** **1999;201):33-40**

(55) **Faerber G, Barreto-Perreia F, Schoepe M, Gilsbach R, Schrepper A, Schwarzer M, Mohr FW, Hein L, Doenst T. Induction of heart failure by minimally invasive aortic constriction**

in mice: reduced peroxisome proliferator-activated receptor gamma coactivator levels and mitochondrial dysfunction. ***J Thorac Cardiovasc Surg.*** **2011;141:492-500**

(56) Laforet P, Inoue M, Goillot E, Lefeuvre C, Cagin U, Streichenberger N, Leonard-Louis S, Brochier G, Madelaine A, Labasse C, et al. Deep morphological analysis of muscle biopsies from type III glycogenesis (GSDIII), debranching enzyme deficiency, revealed stereotyped vacuolar myopathy and autophagy impairment. ***Acta Neuropathol Commun.*** **2019;7:167**

(57) Lang RM, Badano LP, Mor-Avi V, Afilalo J, Armstrong A, Ernande L, Flachskampf FA, Foster E, Goldstein SA, Kuznetsova T, et al. Recommendations for cardiac chamber quantification by echocardiography in adults: an update from the American Society of Echocardiography and the European Association of Cardiovascular Imaging. ***Eur Heart J Cardiovasc Imaging.*** **2015;16:233-70**

(58) Mukherjee A, Srere PA, Frenkel EP. Studies of the mechanism by which hepatic citrate synthase activity increases in vitamin B12 deprivation. ***J Biol Chem.*** **1976;251:2155-60**

(59) Samartsev VN, Chezganova SA, Polishchuk LS, Paydyganov AP, Vidyakina OV, Zeldi IP. Temperature dependence of rat liver mitochondrial respiration with uncoupling of oxidative phosphorylation by fatty acids. Influence of inorganic phosphate. ***Biochemistry (Mosc).*** **2003;68:618-26**

(60) Schwarzer M, Schrepper A, Amorim PA, Osterholt M, Doenst T. Pressure overload differentially affects respiratory capacity in interfibrillar and subsarcolemmal mitochondria. ***Am J Physiol Heart Circ Physiol.*** **2013;304:H529-H537**

(61) Schwarzer M, Osterholt M, Lunkenbein A, Schrepper A, Amorim P, Doenst T. Mitochondrial reactive oxygen species production and respiratory complex activity in rats with pressure overload-induced heart failure. ***J Physiol.*** **2014;592:3767-82**

Novelty and Significance

What Is Known?

- The diaphragm is the main inspiratory muscle responsible for normal ventilation.
- In chronic heart failure (CHF), diaphragm weakness is associated with a worse prognosis; however, we have limited understanding of the basic molecular mechanisms with most of the data derived from animal studies.

What New Information Does This Article Contribute?

- Clinical, functional (*in vivo*/*in vitro*), histological/ultrastructural and molecular alterations of diaphragm biopsies from CHF patients receiving a left ventricular assist device were compared to biopsies of patients without CHF undergoing elective coronary bypass grafting (control).
- NADPH oxidase isoform Nox2 and Nox4 expression was increased in CHF accompanied by catabolic activation and reduced cross-sectional area of type-I and type-II fibers, whereas mitochondria exhibited functional and ultrastructural abnormalities characterized by inhibited autophagy/mitophagy.
- Molecular measures were associated with a clinically evident respiratory muscle dysfunction and reduced whole body exercise capacity in CHF.

Diaphragm weakness in CHF is both responsible for aggravated symptoms and is associated with a worse prognosis. The molecular mechanisms in humans with CHF are poorly understood and, therefore, specific treatment options are lacking. Our data derived from i*n vivo* measures and molecular analyses of diaphragm biopsies revealed that CHF patients suffers from a diaphragm myopathy that occurs independent of disuse or other confounding factors such as ageing, obesity, or hypertension. Specifically, we confirm that severe cellular remodeling and molecular alterations including fiber atrophy, oxidative stress, proteasome-linked catabolic activation, mitochondrial dysfunction, and impaired Ca^{2+} homeostasis underpin diaphragm weakness and wasting in CHF. Clinically, the molecular alterations closely correlate to both whole-body exercise capacity and respiratory function. Thus, our data reveal, for the first time in humans with heart failure, a molecular mechanism and potential therapeutic target for diaphragm weakness that is centered around a cross-talk of NADPH oxidase derived oxidative stress, catabolic activation via the ubiquitin-proteasome system, quantitative and qualitative mitochondrial disturbances and altered Ca^{2+} signaling.

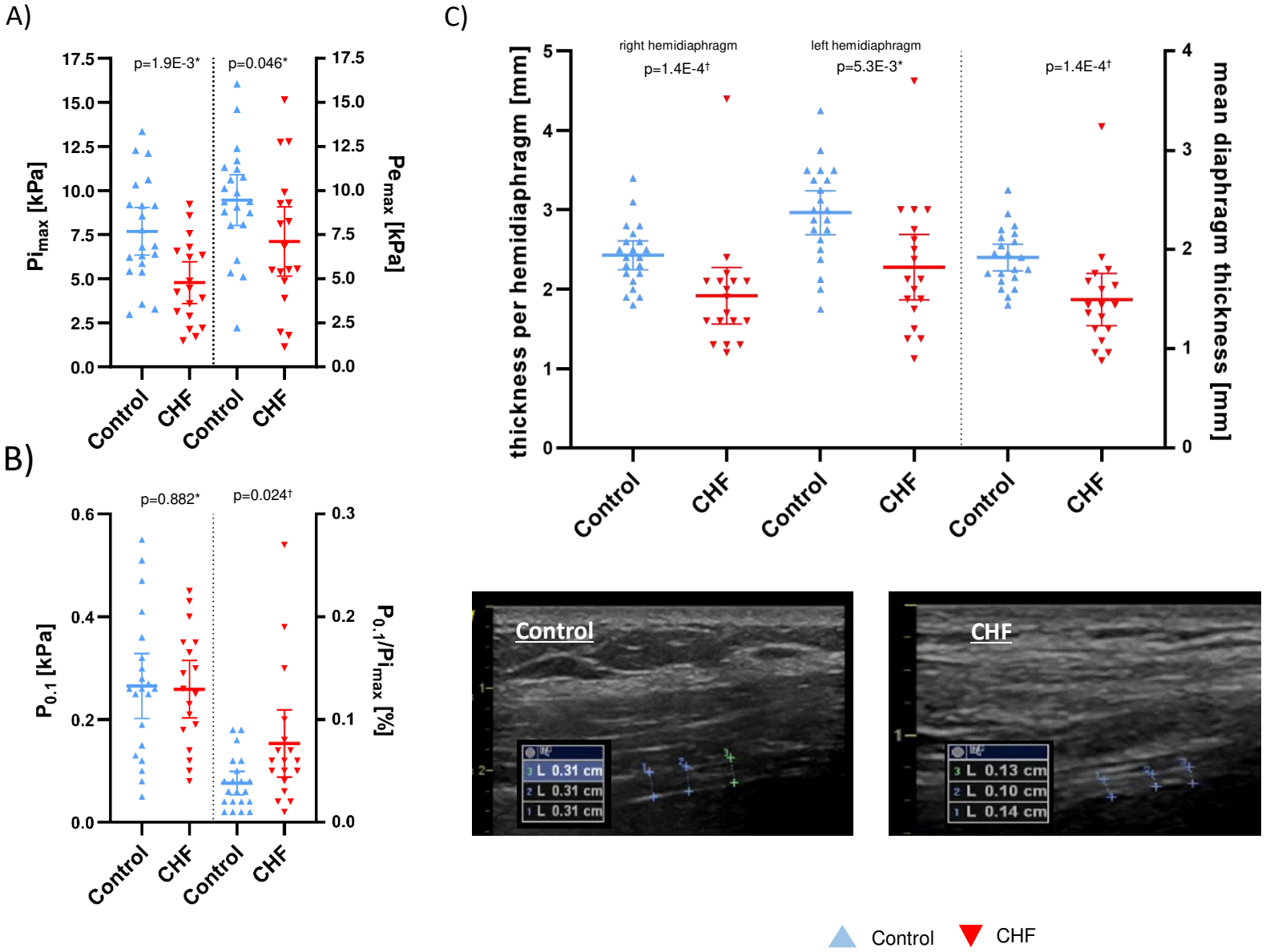
A)
p=1.9E-3*
p=0.046*
Pimax [kPa]
Pemax [kPa]
Control
CHF
Control
CHF
B)
p=0.882*
p=0.024†
P0.1 [kPa]
P0.1/Pimax [%]
Control
CHF
Control
CHF
C)
right hemidiaphragm
p=1.4E-4†
left hemidiaphragm
p=5.3E-3*
p=1.4E-4†
thickness per hemidiaphragm [mm]
mean diaphragm thickness [mm]
Control
CHF
Control
CHF
Control
CHF
Control
L 0.31 cm
L 0.31 cm
L 0.31 cm
CHF
L 0.13 cm
L 0.10 cm
L 0.14 cm
Control
CHF

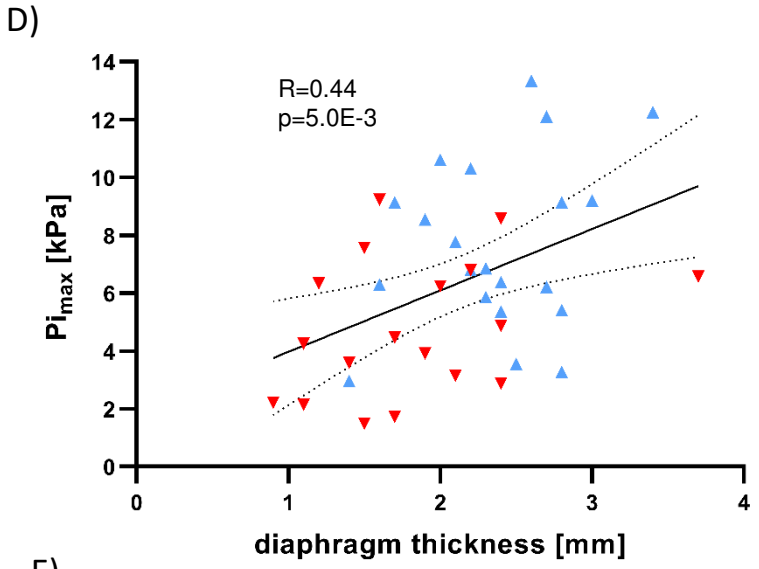
D)
R=0.44
p=5.0E-3
Pimax [kPa]
diaphragm thickness [mm]

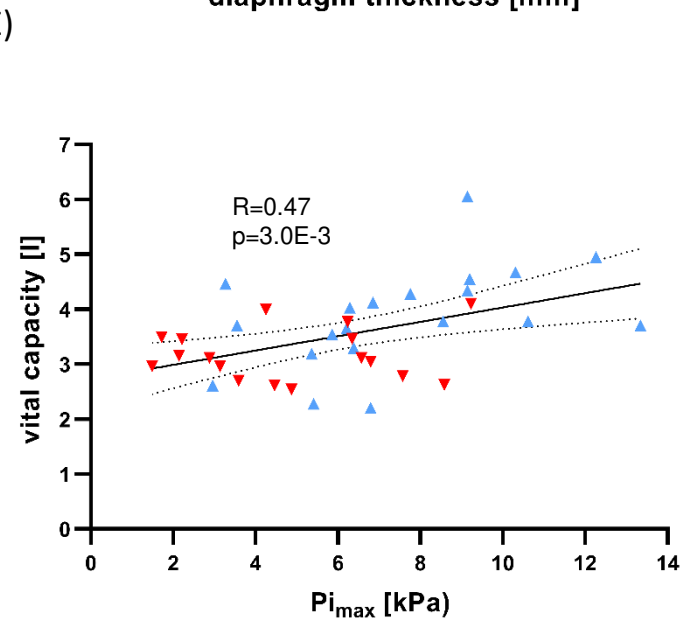
E)
R=0.47
p=3.0E-3
vital capacity [l]
Pimax [kPa]

Figure 1

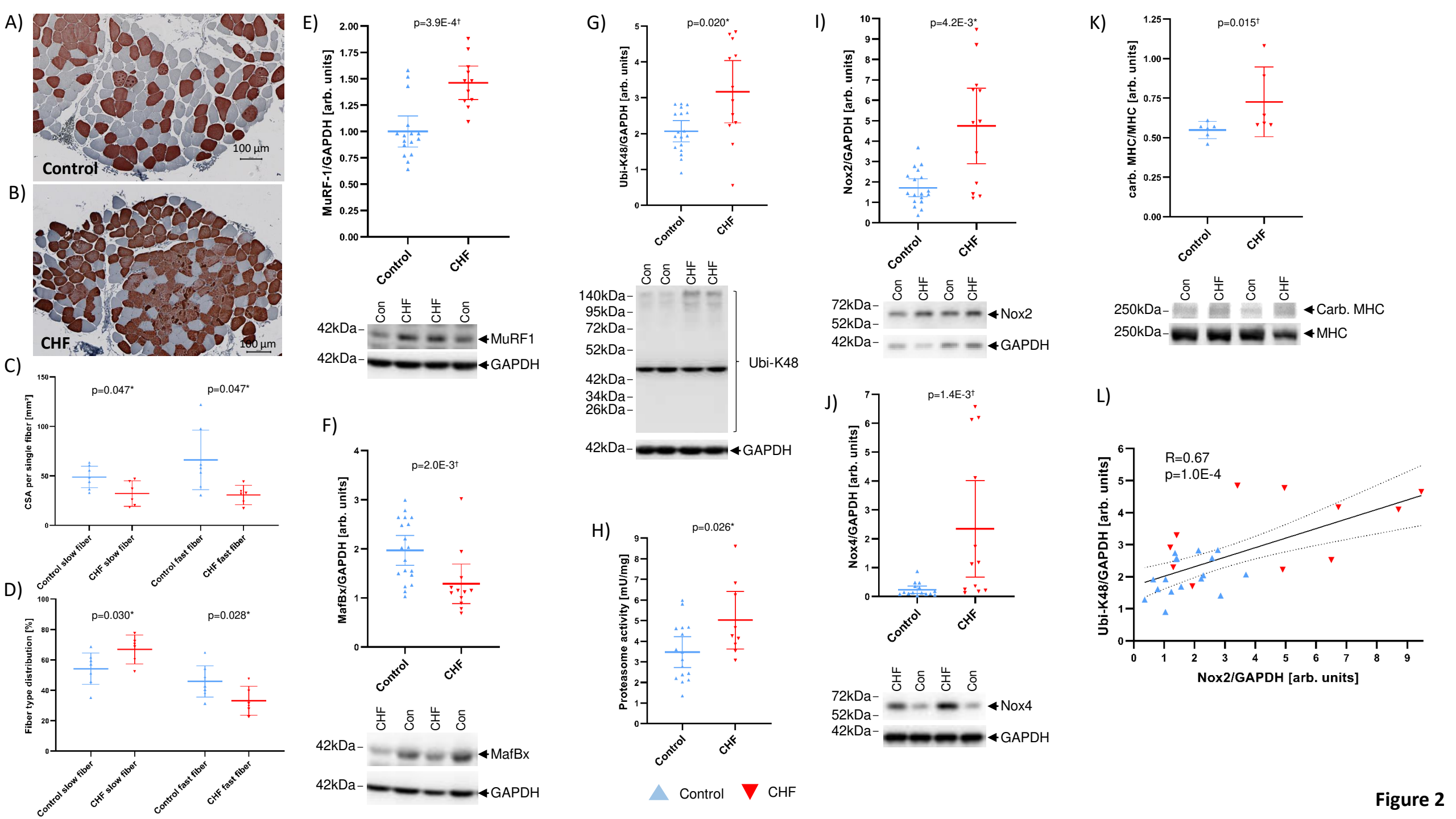
A)
Control
100 µm
B)
CHF
100 µm
C)
CSA per single fiber [mm²]
p=0.047*
p=0.047*
Control slow fiber
CHF slow fiber
Control fast fiber
CHF fast fiber
D)
Fiber type distribution [%]
p=0.030*
p=0.028*
Control slow fiber
CHF slow fiber
Control fast fiber
CHF fast fiber
E)
MuRF-1/GAPDH [arb. units]
p=3.9E-4†
Control
CHF
Con
CHF
CHF
Con
42kDa
MuRF1
42kDa
GAPDH
F)
MafBx/GAPDH [arb. units]
p=2.0E-3†
Control
CHF
CHF
Con
CHF
Con
42kDa
MafBx
42kDa
GAPDH
G)
Ubi-K48/GAPDH [arb. units]
p=0.020*
Control
CHF
Con
Con
CHF
CHF
140kDa
95kDa
72kDa
52kDa
42kDa
34kDa
26kDa
Ubi-K48
42kDa
GAPDH
H)
Proteasome activity [mU/mg]
p=0.026*
Control
CHF
Control
CHF
I)
Nox2/GAPDH [arb. units]
p=4.2E-3*
Control
CHF
Con
CHF
Con
CHF
72kDa
52kDa
42kDa
Nox2
GAPDH
J)
Nox4/GAPDH [arb. units]
p=1.4E-3†
Control
CHF
CHF
Con
CHF
Con
72kDa
52kDa
42kDa
Nox4
GAPDH
K)
carb. MHC/MHC [arb. units]
p=0.015†
Control
CHF
Con
CHF
Con
CHF
250kDa
250kDa
Carb. MHC
MHC
L)
Ubi-K48/GAPDH [arb. units]
R=0.67
p=1.0E-4
Nox2/GAPDH [arb. units]

Figure 2

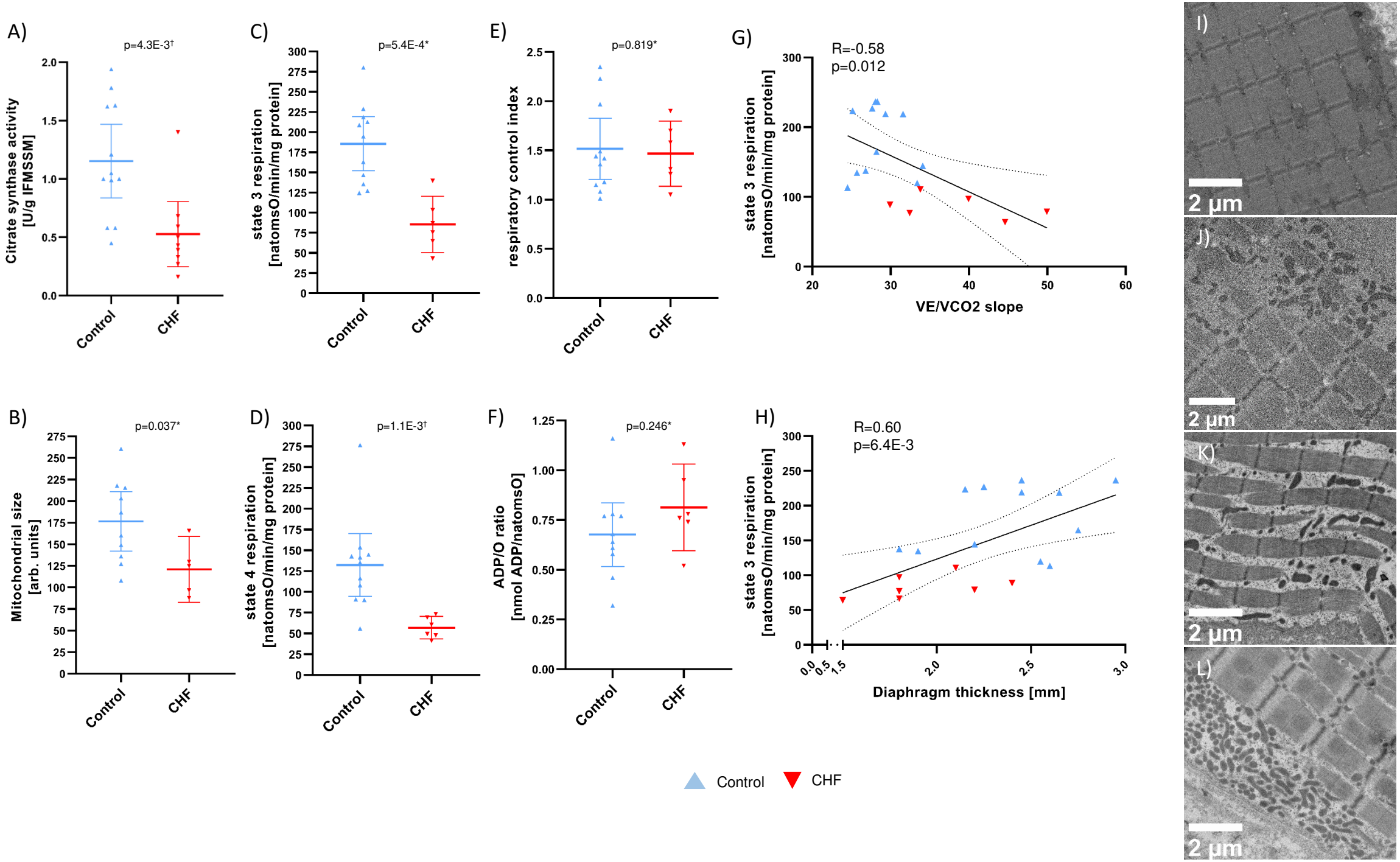
A)
p=4.3E-3†
Citrate synthase activity [U/g IFMSSM]
Control
CHF
C)
p=5.4E-4*
state 3 respiration [natomsO/min/mg protein]
E)
p=0.819*
respiratory control index
G)
R=-0.58
p=0.012
state 3 respiration [natomsO/min/mg protein]
VE/VCO2 slope
B)
p=0.037*
Mitochondrial size [arb. units]
D)
p=1.1E-3†
state 4 respiration [natomsO/min/mg protein]
F)
p=0.246*
ADP/O ratio [nmol ADP/natomsO]
H)
R=0.60
p=6.4E-3
state 3 respiration [natomsO/min/mg protein]
Diaphragm thickness [mm]
Control
CHF
I)
2 µm
J)
2 µm
K)
2 µm
L)
2 µm

Figure 3

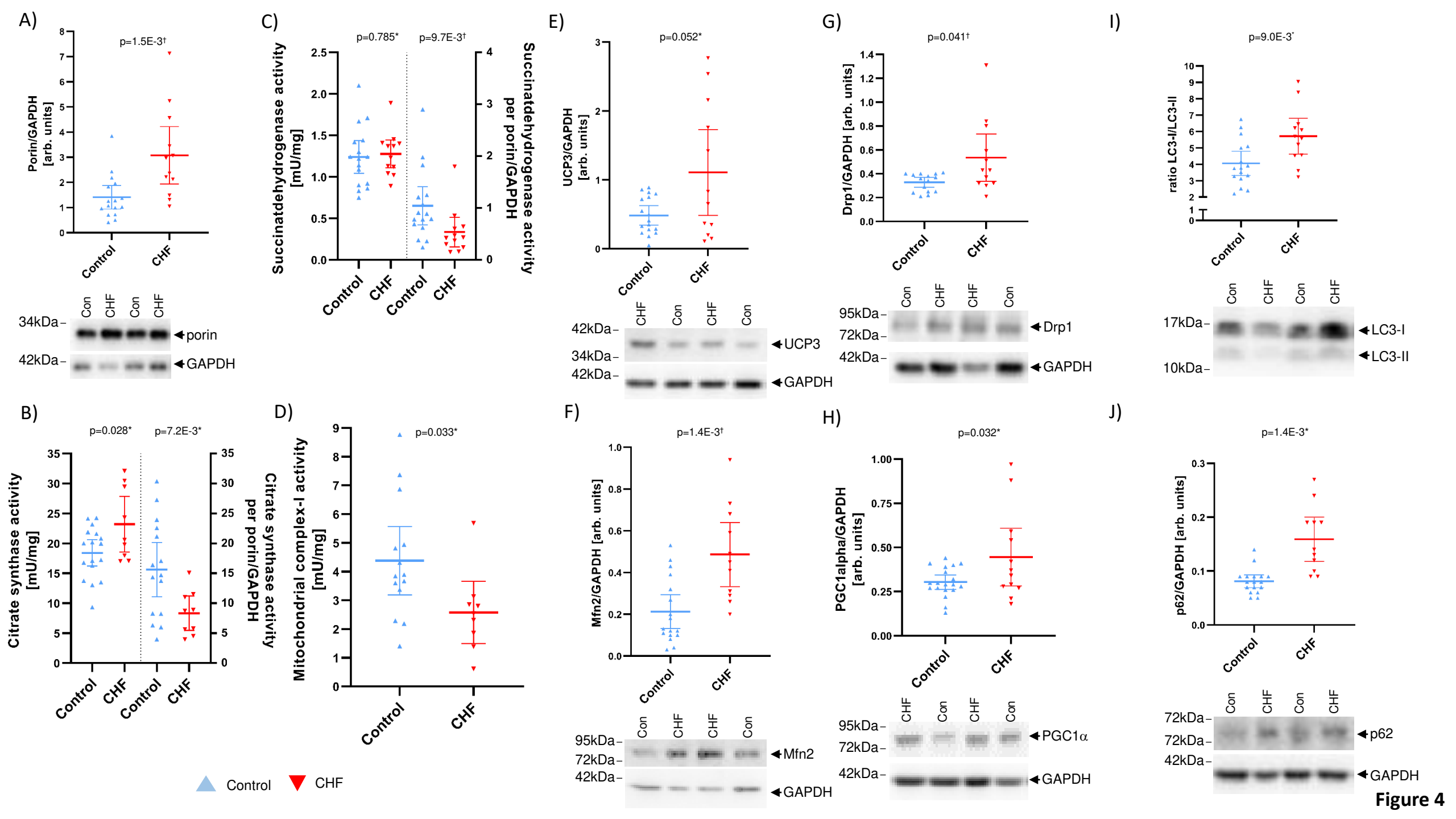
A)
p=1.5E-3†
Porin/GAPDH [arb. units]
Control
CHF
Con
CHF
Con
CHF
34kDa
porin
42kDa
GAPDH
C)
p=0.785*
p=9.7E-3†
Succinatdehydrogenase activity [mU/mg]
Succinatdehydrogenase activity per porin/GAPDH
Control
CHF
Control
CHF
E)
p=0.052*
UCP3/GAPDH [arb. units]
Control
CHF
CHF
Con
CHF
Con
42kDa
UCP3
34kDa
42kDa
GAPDH
G)
p=0.041†
Drp1/GAPDH [arb. units]
Control
CHF
Con
CHF
CHF
Con
95kDa
72kDa
Drp1
42kDa
GAPDH
I)
p=9.0E-3*
ratio LC3-I/LC3-II
Control
CHF
Con
CHF
Con
CHF
17kDa
LC3-I
10kDa
LC3-II
B)
p=0.028*
p=7.2E-3*
Citrate synthase activity [mU/mg]
Citrate synthase activity per porin/GAPDH
Control
CHF
Control
CHF
D)
p=0.033*
Mitochondrial complex-I activity [mU/mg]
Control
CHF
F)
p=1.4E-3†
Mfn2/GAPDH [arb. units]
Control
CHF
Con
CHF
CHF
Con
95kDa
72kDa
Mfn2
42kDa
GAPDH
H)
p=0.032*
PGC1alpha/GAPDH [arb. units]
Control
CHF
CHF
Con
CHF
Con
95kDa
72kDa
PGC1α
42kDa
GAPDH
J)
p=1.4E-3*
p62/GAPDH [arb. units]
Control
CHF
Con
CHF
Con
CHF
72kDa
72kDa
p62
42kDa
GAPDH
Control
CHF

Figure 4

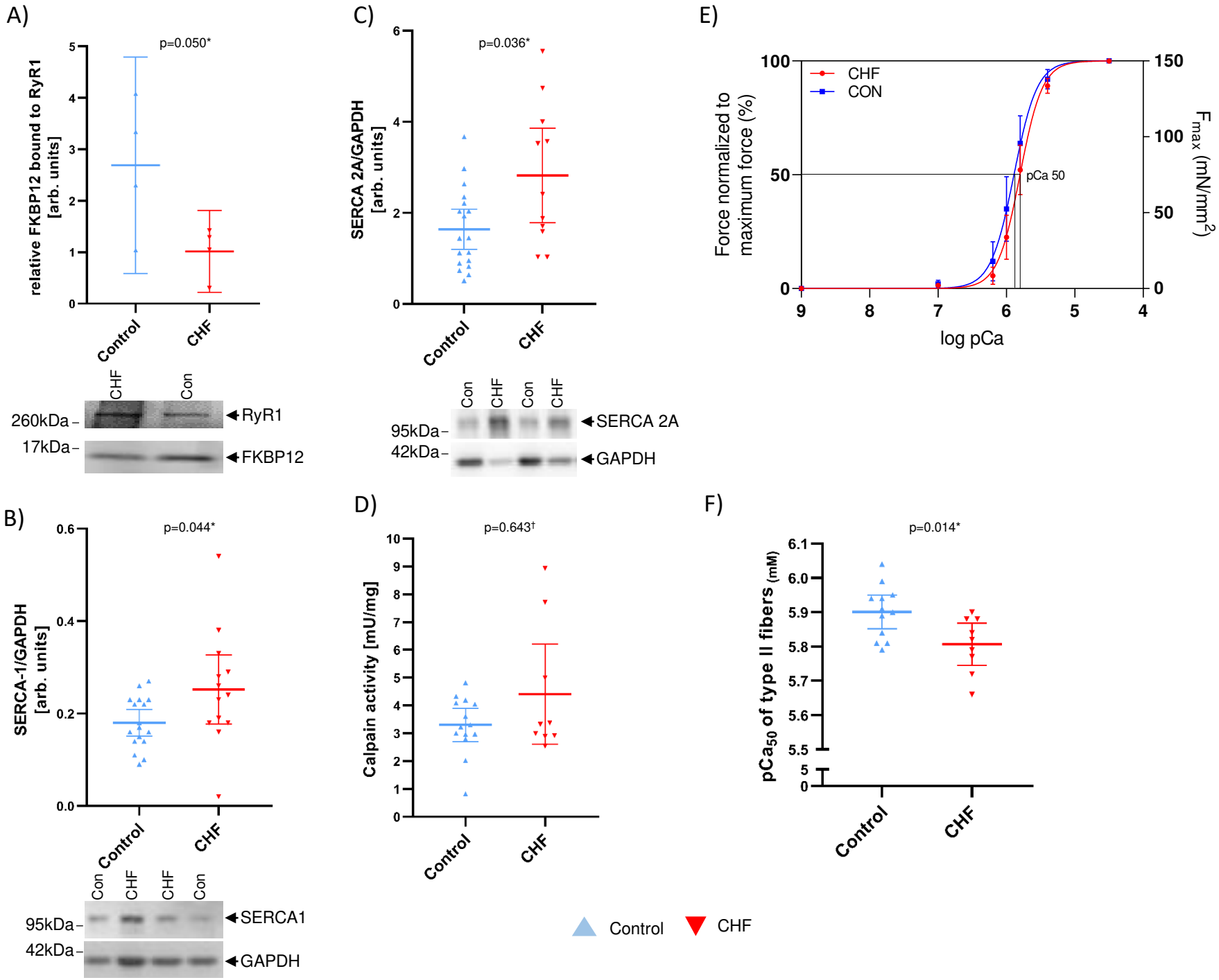
A)
p=0.050*
relative FKBP12 bound to RyR1 [arb. units]
Control
CHF
CHF
Con
260kDa
RyR1
17kDa
FKBP12
C)
p=0.036*
SERCA 2A/GAPDH [arb. units]
Control
CHF
Con
CHF
Con
CHF
95kDa
SERCA 2A
42kDa
GAPDH
E)
CHF
CON
Force normalized to maximum force (%)
pCa 50
log pCa
Fmax (mN/mm2)
B)
p=0.044*
SERCA-1/GAPDH [arb. units]
Control
CHF
Con
CHF
CHF
Con
95kDa
SERCA1
42kDa
GAPDH
D)
p=0.643†
Calpain activity [mU/mg]
Control
CHF
F)
p=0.014*
pCa50 of type II fibers (mM)
Control
CHF
Control
CHF

Figure 5

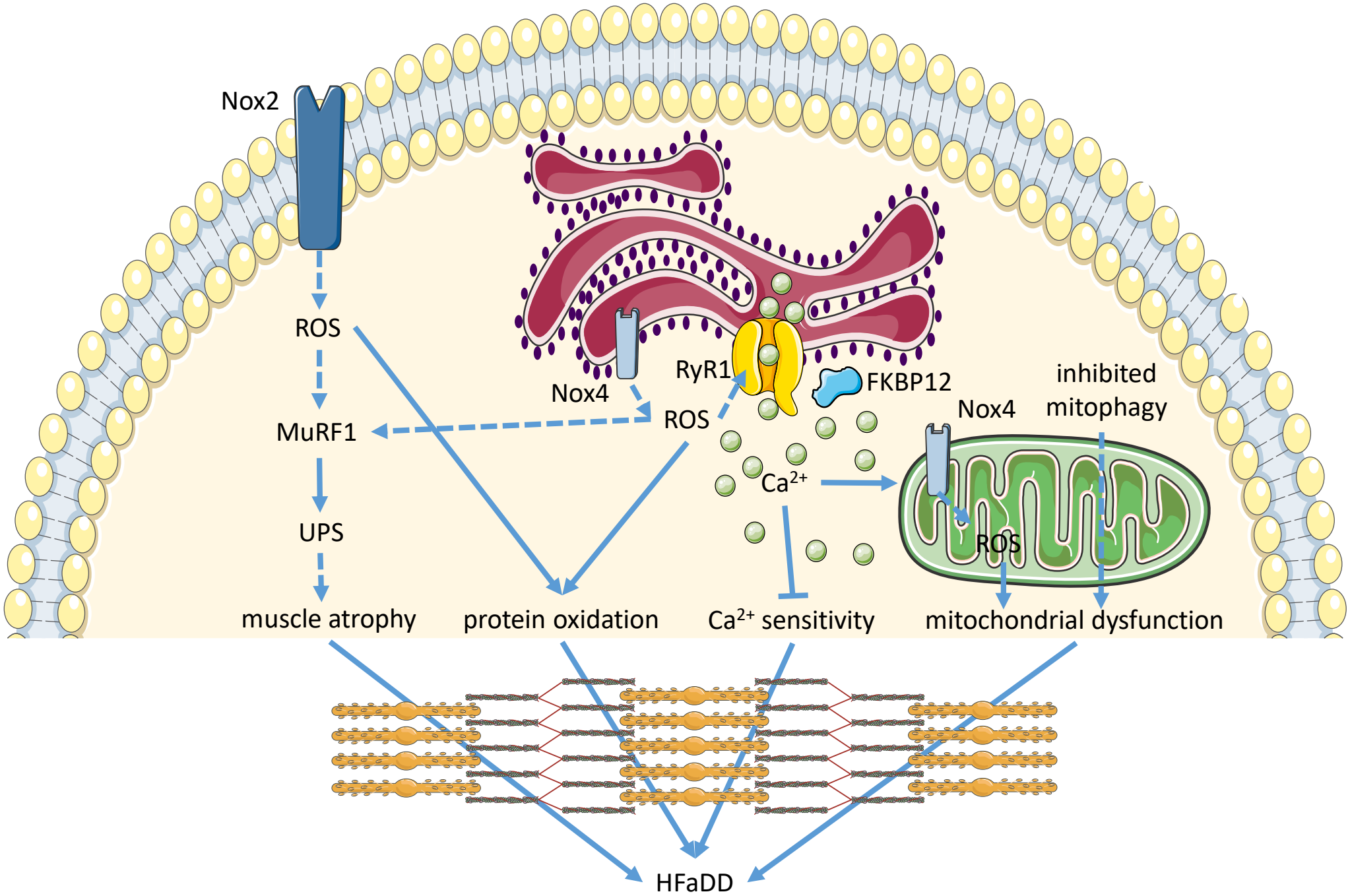
Nox2
ROS
MuRF1
UPS
muscle atrophy
Nox4
RyR1
FKBP12
ROS
protein oxidation
Ca2+
Ca2+ sensitivity
Nox4
inhibited
mitophagy
ROS
mitochondrial dysfunction
HFaDD

Figure 6